

# C-H bonds in Carbon Nanotubes as an Energy Carrier

## Progress report 2011

### Investigators

Principal Investigators: Anders Nilsson (SSRL), Bruce Clemens (Materials Science and Engineering), Hongjie Dai (Chemistry)

Hirohito Ogasawara (staff scientist, SSRL), Daniel Friebe (Research Associate, SSRL), Srivats Rajasekaran (PhD student, Materials Science and Engineering), Liying Jiao (postdoc, Chemistry), Cara Beasley (Graduated, Chemistry), Ranadeep Bhowmick (Graduated, Material Science and Engineering)

### Abstract

We investigate the capability of single-walled carbon nanotubes (SWNT) as a possible material for hydrogen storage through the reversible formation of stable C-H bonds. While SWNTs have been successfully hydrogenated in our previous studies using an atomic hydrogen source, we are currently pursuing two possible low-energy hydrogenation pathways, which both employ the concept of “spillover” of H atoms from a Pt catalyst; H atoms can be generated either by electrochemical reduction of  $H^+$  from aqueous electrolyte, or by catalytic dissociation of molecular hydrogen. Using a combination of *in situ* electrical conductivity and *ex situ* x-ray photoelectron spectroscopy (XPS) measurements, we have examined how the hydrogen uptake of single-walled carbon nanotubes (SWNTs) is influenced by the addition of Pt nanoparticle catalyst. The conductivity of platinum-sputtered single-walled carbon nanotubes (Pt-SWNTs) decreased rapidly during hydrogen exposure, which supports a hydrogenation mechanism facilitated by spillover of dissociated hydrogen from the Pt nanoparticles. C 1s XPS spectra taken after hydrogen exposure show a significant amount of carbon atoms in the  $sp^3$  hybridized state due to covalent C-H bond formation. Hydrogen charging at elevated pressure (8.27 bar) and room temperature of particular set of Pt-SWNT composites yielded hydrogen-storage capacity of 1.2 wt.% (excluding the weight of Pt nanoparticles).

A major challenge in achieving significant hydrogen uptakes is the fabrication of a composite where the surface area is high and each individual nanotube is in direct contact with

Pt. We have made significant progress towards preventing individual tubes from forming bundles; this allows for more efficient Pt loading and higher hydrogen capacity.

An electrochemical cell was developed to explore electrochemical pathways towards hydrogenation through spillover process, which will be probed with *in situ* x-ray Raman scattering (XRS).

## **Introduction**

Previous studies have indicated that it is possible to approach hydrogen storage capacities of 5-6 wt.% in SWNTs through treatment with an atomic hydrogen source through formation of C-H bonds.<sup>1</sup> But practical implementation of hydrogen storage in SWNTs requires the development of low-barrier pathways for hydrogen dissociation. One potential pathway could be the “spillover” mechanism, in which molecular hydrogen spontaneously dissociates on a transition metal catalyst<sup>2</sup> attached to the SWNTs, producing mobile H atoms that spill over onto the SWNTs. However, the validity of the spill-over mechanism and the possibility of significant hydrogen storage in SWNTs remain controversial. Only few studies exist including inelastic neutron-scattering (INS) experiments<sup>3</sup> and isotope exchange TPD experiments<sup>4</sup> performed on metal-carbon composites which favorably suggest the existence of a spillover mechanism. So it is important to obtain a proof of principle for the existence of the spillover mechanism and that it could be exploited for hydrogen storage applications. Once this mechanism is validated, we could explore an electrochemical pathway for hydrogen loading as an alternative to gas phase hydrogen loading. In this report we briefly discuss the hydrogen capacity of Pt-SWNT composites under hydrogen gas exposure and the *in situ* electrochemical cell design, which was developed to probe the carbon hybridization state during electrochemical operation using XRS. The hydrogen capacity of Pt-SWNT composites depend strongly on the size of the catalyst particle and the morphology of the nanotubes used. In general, SWNTs with maximum catalyst particle density showed maximum hydrogen storage capacity. Part of the gas exposure loading and the corresponding conductivity measurements were discussed in previous year’s report.

## **Individual Single-Walled Carbon Nanotubes for Hydrogen Storage Applications (Dai group)**

**Separation and spectroscopy investigations of individual SWNTs.** Single-walled carbon nanotubes (SWNTs) are a unique class of macromolecule, conceptualized as a single graphitic sheet of  $sp^2$  carbon atoms, rolled into a seamless cylinder, with diameters of  $\sim 0.5 - 1.6$  nm, and lengths from tens of nanometers up to millimeters. For various applications of nanotubes, it is necessary to obtain individual SWNTs rather than bundled nanotubes, to maximize the surface area for applications such as hydrogen storage and optimize the physical properties of nanotubes such as photoluminescence and resonance raman scattering.

Unfortunately, as-grown SWNTs are heavily bundled. The Dai group set out to obtain purely individual SWNT samples desired for hydrogen storage. We used density gradient centrifugation (DGC) rate (zonal) separation for sodium-cholate suspended SWNTs through an iodixanol step-gradient at  $\sim 300,000$  g. This method separates nanotubes by mass, with fractions rich in single tubes floating on top of the column and bundles settling at the lower parts of the centrifuge column.

Resonance Raman scattering analysis, under 785 nm laser excitation, of the DGC separated SWNT fractions showed similar intensity trends as the relative photoluminescence (PL) measurements, for both the radial breathing modes (RBMs) and graphitic band (G-band). The DGC separated and absorbance-normalized fractions of SWNTs showed a sharp rise in Raman scattering intensity from fractions 3-6, with a peak in both the RBM and G-band scattering intensity in fraction 6, coinciding with the peak in PL QY. This peak is followed by a gradual decrease in intensity for both modes.

The cause of the gradual loss of both PL QY and Raman scattering intensity in higher fractions is due to presence of small nanotube bundles. Bundling of dispersed SWNTs is known to reduce PL QY via non-radiative energy transfer processes. Excitons can decay non-radiatively into a neighboring metallic nanotube, leading to quenching of the photoluminescence. Bundling also causes red-shifting and absorption peak broadening of the excitonic optical transitions in SWNTs. We observed a red-shift of 13 nm (25 meV) for the optical transition near 800 nm with increasing fraction number. Broadening of optical transition peaks was also observed, suggesting the presence of a broad distribution in the degree of SWNT bundling. Indeed, Raman scattering analysis revealed an increase in (10,2) RBM intensity indicating an increase in SWNT bundling following DGC, in fraction 7 and above.

The decrease in Raman scattering intensity in higher fractions is related to the red-shifting of the SWNT optical transitions, following from an increasing proportion of SWNT bundles with increasing fraction number. Bundling of SWNTs, perturbs the SWNT single-particle band structure and increases dielectric screening effects, which in turn reduce excitonic optical transitions. This effect is in part mitigated by a decrease in exciton binding energies, but overall the band structure effects outweigh excitonic effects. Charge transfer, caused either by interactions of SWNT sidewalls or the  $\pi$ -density contribution of small aromatic molecules, leads to increased coulomb interactions, and subsequent carrier charge screening, that reduces exciton lifetimes, and leads to PL quenching and contributes to the broadening of optical transitions.

In conclusion, the Dai group has performed density gradient centrifugation (DGC) of sodium cholate-suspended SWNTs in water to separate individual nanotubes from small bundles. Long, individual SWNTs exhibit the highest PL and Raman scattering intensities, 2- to 4-fold higher than as-made SWNT suspensions containing both single and bundled carbon nanotubes. SWNTs found located in high-numbered fractions had higher degrees of bundling, resulting in increasingly red shifted and broadened absorption peaks. This is the first time that a systematic investigation is carried out with separated nanotubes to correlate the photoluminescence, resonance Raman scattering, and optical absorption of individualized versus small, bundled nanotubes. Importantly, our method obtains fractions of highly individualized nanotubes, useful for various applications.

The Dai group has made SWNT film for hydrogen storage studies for this grant. Uniform monolayer of unbundled SWNTs was obtained for the highest loading with Pt and therefore the highest hydrogen-storage capacity on a weight-percent basis. We used individual tubes extracted in this manner to prepare monolayer assemblies of SWNT films by the Langmuir-Blodgett (LB) method, in which SWNTs functionalized by PmPV were dispersed in 1,2-dichloroethane. We calcined the LB films to remove organic solvents, surfactants, and any other remaining contaminants for of Pt coating and hydrogen spill over studies.

In summary, we have performed density gradient centrifugation (DGC) of sodium cholate-suspended SWNTs in water to separate individual nanotubes from small bundles. Long, individual SWNTs are obtained based on spectroscopy measurements. Our method obtains

fractions of highly individualized nanotubes, which are now available for hydrogen storage experiments. However, a major next hurdle is to scale up such individual SWNTs to large quantities needed for future realistic storage applications.

### Gas phase hydrogen loading - *in situ* conductivity measurements (Clemens group)

The SWNT samples used were (a) CVD-grown (b) HiPCO samples dispersed employing a combination of nanotube unbundling via density-gradient centrifugation and film deposition using the Langmuir-Blodgett method (LB) and (c) commercial HiPCO samples. The details of the sample preparation are described in our annual report from 2010. The SWNT samples were sputtered with Pt nanoparticles to make Pt-SWNT composites. Pt-SWNT composites with different nominal thickness of sputtered Pt were used in conductivity studies to understand the influence of catalyst size on hydrogen storage capacity. Details about *in situ* 4-probe resistance measurements under hydrogen gas exposure have been described in our previous annual report.

The resistance measurements were performed under systematic variation of the following parameters: the amount of Pt loading (Fig. 1, 2a), the density of SWNT films (Fig. 2b), and the temperature during hydrogen exposure (Fig. 3).

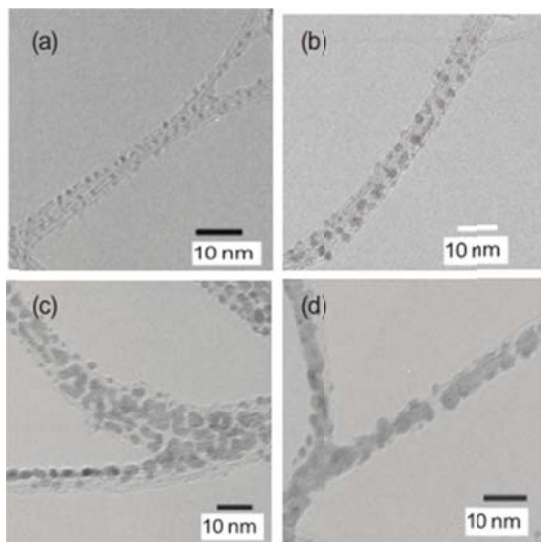


Fig. 1. Evolution of Pt nanoparticle sizes on SWNTs with increasing nominal thickness of deposited Pt (a) 0.2 nm (b) 0.5 nm (c) 1 nm (d) 3 nm.

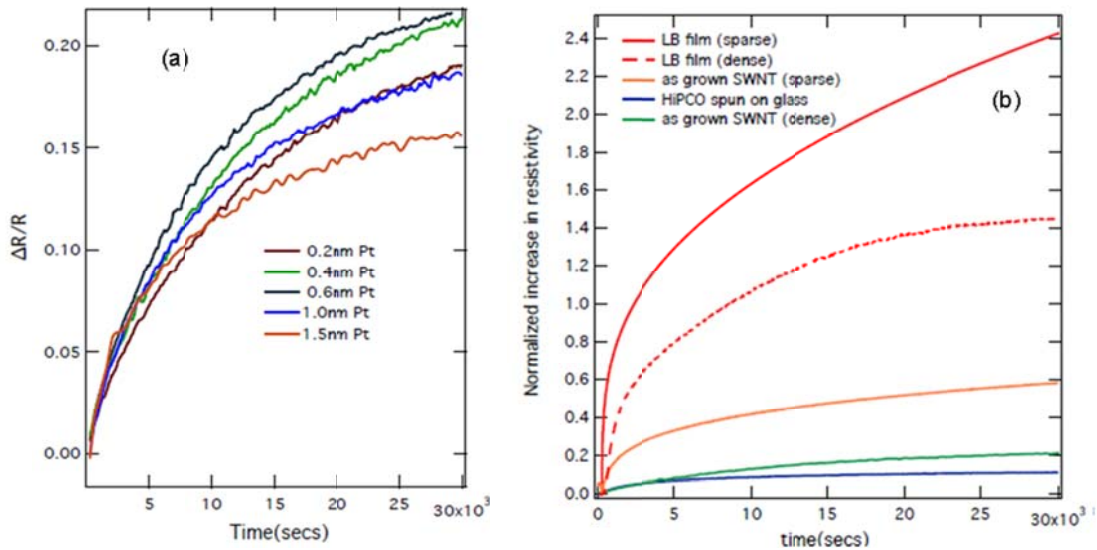


Fig. 2. Normalized resistance change for Pt-SWNTs as a function of exposure time at 700 torr hydrogen gas, (a) using different amounts of deposited Pt (in nominal thickness), (b) using different film preparation techniques resulting in different degrees of SWNT bundling.

TEM micrographs of HiPCO samples with different amounts of deposited Pt are shown in Fig. 1. It could be observed from TEM micrographs that the sputtered Pt film does not wet the SWNT surface but aggregates into particles. The size and distribution of the particles formed depend on the nominal thickness of the sputtered Pt. Increase in nominal thickness of the catalyst particles lead to an increase in normalized resistance to an optimal level, beyond which decrease of normalized resistance was observed (Fig. 2a). The optimal thickness of the deposited Pt film is 0.6 nm (particle diameter  $\sim(2.05 \pm 0.36)$  nm). The TEM micrographs indicate that with an increase in the nominal thickness of the Pt film, the density as well as the size of the catalyst particles increases. Beyond a certain thickness of sputtered film, the Pt particles start agglomerating, thus decreasing the number density of the particles and hence decreasing the extent of possible H spillover onto the SWNT surface. Nominal thickness increase from 0.2 nm to 0.6 nm resulted in an increase in number density of Pt nanoparticles on the SWNTs with slight increase in particle size. Around nominal thickness of 1 nm, reduction in the number density of Pt nanoparticles was observed due to agglomeration of large particles. Hence, the Pt coverage that yields the highest number density of catalyst particles has the highest storage capacity potential. This optimal thickness for maximum hydrogen uptake is in good agreement with hydrogen uptake measurements using a Sieverts apparatus,<sup>5</sup> where it was observed that the

hydrogen uptake by a Pt-SWNT composite film varies linearly with the density of the Pt particles.

The effect of SWNT various sample preparation techniques, which result in different degrees of bundling, on the hydrogen uptake is shown in Fig. 2b. Spin-cast films of HiPCO SWNTs and as-grown films produced using CVD show a strong tendency towards formation of bundles; this makes it difficult to efficiently prepare composites with Pt nanoparticles, where direct contact between each nanotube and Pt is desired. Significantly improved hydrogen uptake could be achieved when we used a CVD procedure that yielded less dense films. The greatest improvement so far has been found with a procedure where unbundled HiPCO SNWTs were isolated using density gradient centrifugation, and subsequently deposited using the Langmuir-Blodgett technique.

It was observed that the resistance plots do not saturate during the time scale of the hydrogenation experiments (8 hours), indicating slow kinetics. We conjecture that diffusion of H over the SWNT surface is rate-limiting in the hydrogenation mechanism. In fact, we found that increasing the temperature increases the initial hydrogen uptake rate and, at temperatures higher than 94 °C, equilibrium can be reached during the timescale of our experiment. On the other hand, the overall change in resistance at any time beyond ~2 h is the largest at -5 °C and decreases monotonically with increasing temperature. Hence, while increased temperatures improve the kinetics of the hydrogen spillover, at the same time the thermodynamic equilibrium is unfavorably shifted, decreasing the hydrogen storage capacity.

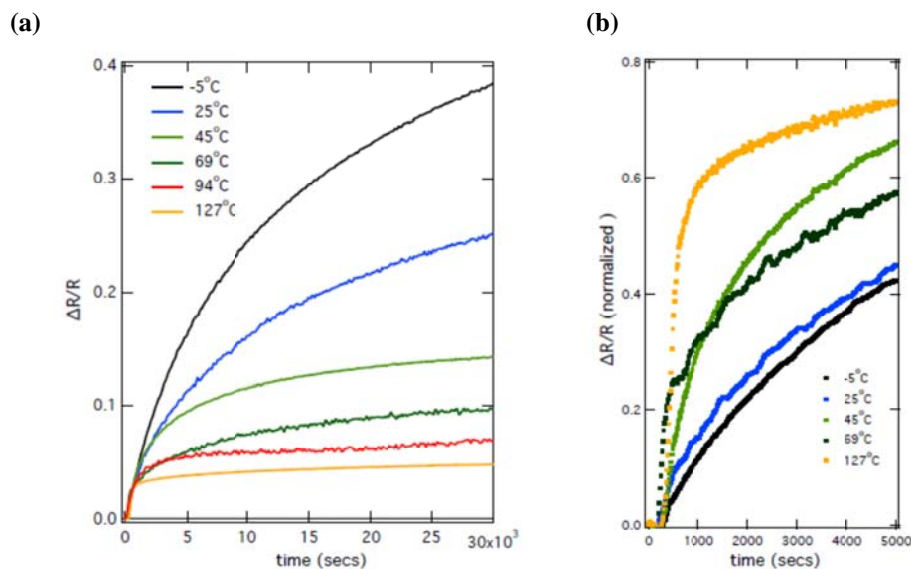


Fig. 3. (a) Hydrogen uptake measured at different temperatures, (b) enlarged plot showing the initial behavior.

### **Direct evidence for C–H bond formation: XPS studies (Nilsson group)**

In order to verify that the changes observed in conductance measurements are indeed due to hydrogenation, XPS measurements of CVD-grown (CVD) and LB-film samples with a nominal 0.6nm thickness of deposited Pt were performed before and after hydrogen exposure (8.27 bar H<sub>2</sub> at room temperature for 3 hours). The incident x-ray energy was set to  $h\nu_{in} = 400$  eV. The C 1s spectra are shown in Fig. 4 and Fig. 5, with the binding energy referenced to the Fermi level. The full-width at half-maximum (FWHM) of the C 1s peak before hydrogen loading is 1.4 and 1.15 eV for the CVD-grown SWNTs (Fig. 4a) and LB films (Fig. 5a), respectively. For both the CVD-grown and LB-film composites, the spectra acquired before hydrogen exposure can be fitted with a single asymmetric Gaussian-Lorentzian (GL) component centered at 284.8 eV (Fig. 4b and 5b), corresponding with  $sp^2$ -hybridization of the C atoms; the asymmetric tail of these spectra can be attributed to electron-hole pair excitations at the Fermi level arising from the metallic nature of the CNTs. After exposure to hydrogen at a pressure of 8.27 bar for 6 hours, the FWHM of the C 1s spectrum of the CVD-grown SWNTs increased to 1.5 eV (Fig. 4(a)), while that of the LB films increased to 1.35 eV (Fig. 5(a)). Peak fitting reveals a new feature in addition to the previously observed  $sp^2$ -peak, which we fitted using a symmetric GL with 2 eV FWHM. This new spectral contribution is assigned to C atoms that have undergone rehybridization from  $sp^2$  to  $sp^3$  due to the breaking of C–C  $\pi$ -bonds and C–H bond formation,<sup>1</sup> and can be seen as a direct evidence for the proposed spillover effect.

An additional peak at 288 eV (shifted by  $\sim 3.3$  eV from the main  $sp^2$  C1s peak) can be detected for hydrogenated samples. A similar feature was observed when pure SWNTs were treated with atomic hydrogen.<sup>6</sup> We conjecture that this additional peak arises from a metal-to-semiconductor transition of the nanotubes that is induced by hydrogenation. The decrease in conductivity accompanying such a transition can cause a reduction of the core-hole screening that increases the final-state energy by  $\sim 2$ -3 eV. The hydrogen uptake due to exposure to molecular hydrogen of  $\sim 8.27$  bar, quantified by XPS indicates 1.2 wt.% hydrogen storage for LB-film composites and 1 wt.% for CVD-grown CVD composites.

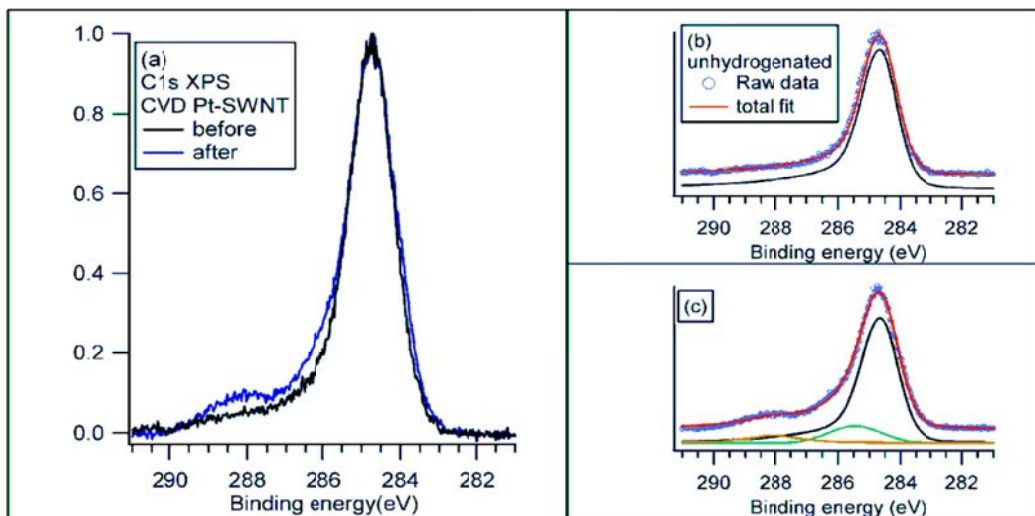


Fig 4. (a) C 1s XPS spectra before (*black*) and after (*blue*) hydrogen charging for CVD-grown film with 0.6nm Pt; the spectra are normalized to peak maxim to enhance differences in the peak shapes. Gaussian-Lorentzian deconvolution (see text for details) (b) before and (c) after hydrogen charging: raw data (*open blue circles*); total fit (*red*);  $sp^2$ -C peak (*black*);  $sp^3$ -C peak (*green*); additional peak due to hydrogen-induced metal-to-semiconductor transition (*orange*). Fits are offset from raw data for clarity.

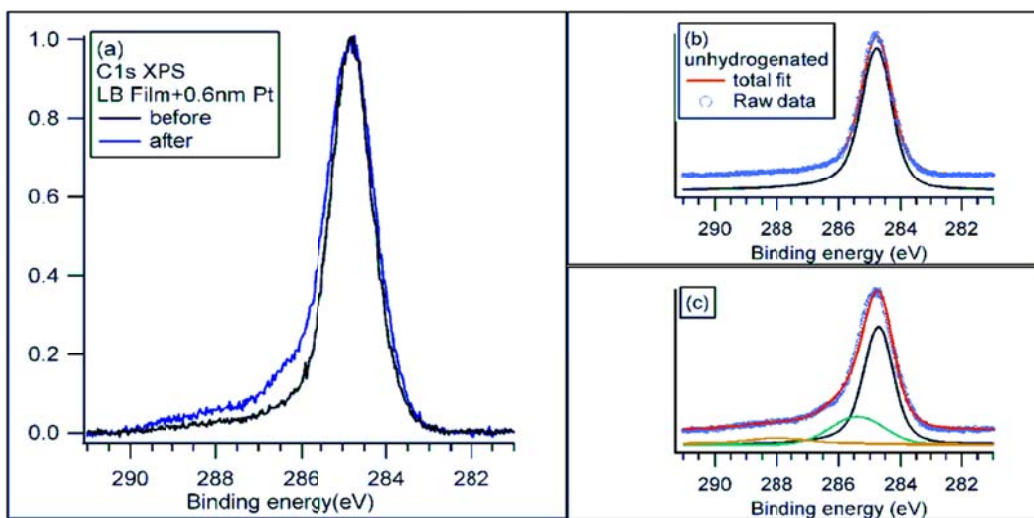


Fig. 5. (a) C 1s XPS spectra before and after hydrogen exposure for an LB film with 0.6nm Pt; the peak maxima of both spectra are normalized to enhance differences in the peak shapes. Gaussian-Lorentzian deconvolution (see text for details) (b) before and (c) after hydrogen charging: raw data (*open blue circles*); total fit (*red*);  $sp^2$ -C peak (*black*);  $sp^3$ -C peak (*green*); additional peak due to hydrogen-induced metal-to-semiconductor transition (*orange*). Fits are offset from raw data for clarity.

## Electrochemical cell for *in situ* x-ray Raman scattering – Design and Future experiments (Nilsson group)

Preliminary results from electrochemical cyclic voltammetry in 0.05M H<sub>2</sub>SO<sub>4</sub> have been shown in previous reports. It was demonstrated that pure CNTs exhibit no voltammetric features other than double layer and hydrogen evolution currents, the latter being shifted significantly to lower potential values by an overpotential of ~0.2 V. For Pt-CNT samples, no significant overpotential is observed for the hydrogen evolution since Pt is a good catalyst for this reaction, and a new anodic peak appears in the positive potential sweep. The anodic peak could be seen as an indication for the oxidation of C–H bonds, but since also the oxidation of H adsorbed at the Pt surface is known to occur in the same potential region, the interpretation of the current-voltage curves alone will not be unambiguous. Hence direct spectroscopic evidence is required to prove the existence of C–H species.

In XRS, photons are scattered inelastically and transfer their energy loss to the excitation of a core electron. Therefore, XRS can, in principle, employ hard x-rays to produce absorption spectra that would usually require incident energies in the soft x-ray regime. Hence, low-Z elements such as C can be probed *in situ* in a liquid-electrolyte environment that would not be accessible to soft x-rays. We will use *in situ* XRS to detect C–H bond formation during electrochemical hydrogenation of Pt-SWNT composites. We expect spectral signatures similar to those that we observed after treating pure SWNTs with atomic hydrogen: a decrease in the  $\pi^*$  resonance due to hydrogenation and the appearance of a C-H  $\sigma^*$  resonance ~3 eV above the  $\pi^*$  resonance. The XRS technique has been successfully employed by other research groups to study changes in the nature of bonding and hybridization in multi-walled carbon nanotubes under high pressures where a transition to a diamond-like structure occurs.<sup>7</sup>

The electrochemical *in situ* XRS cell which will be used to observe possible hydrogenation in Pt-SWNTs is shown in Fig. 6. The cell provides a three-electrode setup with a leak-free Ag/AgCl reference electrode and a Pt counter electrode. The working electrode consists of a ~100 nm thin silicon nitride window that is coated with a ~100 nm Au film to provide electrical conductivity. A Pt-SWNT composite will be cast in a ~1 mm thick layer onto the Au film. This setup will allow for the sample to be illuminated from the back and minimizes the Compton scattering background from the electrolyte and the window materials.

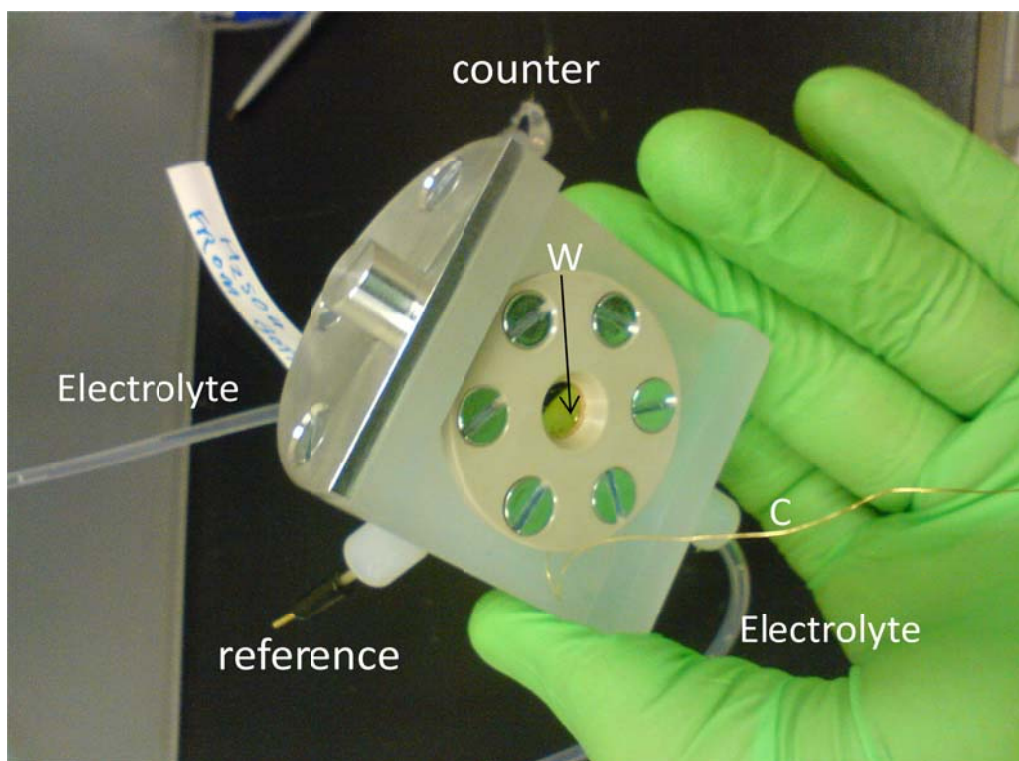


Fig. 6. Electrochemical *in situ* XRS cell, the working electrode is marked with “W”.

## Publications

R. Bhowmick, S. Rajasekaran, D. Friebe, C. Beasley, L. Jiao, H. Ogasawara, H. Dai, B. Clemens, A. Nilsson, “Hydrogen Spillover in Pt-Single-Walled Carbon Nanotube Composites: Formation of Stable C–H Bonds”, *J. Am. Chem. Soc.* **2011**, *133*(14), 5580–5586; doi: 10.1021/ja200403m

## References

- [1] A. Nikitin, H. Ogasawara, D. Mann, R. Denecke, Z. Zhang, H. Dai, A. Nilsson, *Phys Rev Lett.* **2005**, *95*, 225507.
- [2] G. A. Somorjai, *Introduction to Surface Chemistry and Catalysis* Wiley-Interscience, **1994**.
- [3] P. C. H. Mitchell, A. J. Ramirez-Cuesta, S. F. Parker, J. Tomkinson, and D. Thompsett, *J. Phys. Chem. B* **2003** *107* (28), 6838–6845.
- [4] A.J. Lachawiec. Jr, and R.T. Yang, *Langmuir* **2008**, *24* (12), 6159–6165.
- [5] Y-W. Lee, Hydrogen storage properties of catalyst metal-doped single-walled carbon nanotubes, PhD Thesis, Stanford University **2009**.
- [6] A. Nikitin, X. Li, Z. Zhang, H. Ogasawara, H. Dai, A. Nilsson, *Nano Lett.* **2008**, *8* (1), 162–167.
- [7] R. S. Kumar, M. G. Pravica, A. L. Cornelius, M. F. Nicol, M.Y. Hu, P. C. Chow, *Diamond and related materials* **2006**, *16*, 1250-1253.